AEDC-TR-68-99

cy.7

STUDY OF THE BLUNT-BODY STAGNATION POINT VELOCITY GRADIENT IN HYPERSONIC FLOW

L. L. Trimmer

ARO, Inc.

May 1968

VON KÁRMÁN GAS DYNAMICS FACILITY
ARNOLD ENGINEERING DEVELOPMENT CENTER
AIR FORCE SYSTEMS COMMAND
ARNOLD AIR FORCE STATION, TENNESSEE

NOTICES

When U. S. Government drawings specifications, or other data are used for any purpose other than a definitely related Government procurement operation, the Government thereby incurs no responsibility nor any obligation whatsoever, and the fact that the Government may have formulated, furnished, or in any way supplied the said drawings, specifications, or other data, is not to be regarded by implication or otherwise, or in any manner licensing the holder or any other person or corporation, or conveying any rights or permission to manufacture, use, or sell any patented invention that may in any way be related thereto.

Qualified users may obtain copies of this report from the Defense Documentation Center.

References to named commercial products in this report are not to be considered in any sense as an endorsement of the product by the United States Air Force or the Government.

STUDY OF THE BLUNT-BODY STAGNATION POINT VELOCITY GRADIENT IN HYPERSONIC FLOW

L. L. Trimmer
ARO, Inc.

AF - AEDC
Arnold AFS Tenn

FOREWORD

The work reported herein was sponsored by the Arnold Engineering Development Center (AEDC), Air Force Systems Command (AFSC), under Program Element 6540223F.

The results of research presented were obtained by ARO, Inc. (a subsidiary of Sverdrup & Parcel and Associates, Inc.), contract operator of AEDC, AFSC, Arnold Air Force Station, Tennessee, under Contract AF40(600)-1200. The research was conducted under ARO Project No. VT2806, and the manuscript was submitted for publication on April 5, 1968.

The information in this report was also submitted by the author to the University of Tennessee Space Institute in August 1966, in partial fulfillment of the requirements for a Master of Science degree.

This technical report has been reviewed and is approved.

Donald H. Meyer
Major, USAF
AF Representative, VKF
Directorate of Test

Roy R. Croy, Jr.
Colonel, USAF
Director of Test

ABSTRACT

Results of an experimental investigation to determine the stagnation point velocity gradients for a family of blunt axisymmetric shapes at hypersonic Mach numbers are presented. Data presented in the form of model pressure distributions and stagnation point Mach number gradients are compared with existing data and theories. Although not accurately predicting the results, Newtonian theory is shown to provide a good basis for data correlation. Variations in model pressure distribution and stagnation point Mach number gradient from free-stream Mach number 6 to 10 were small and essentially within experimental precision. Model bluntness ranged from a hemisphere-cylinder to a flat-nose-cylinder, and data were obtained at free-stream Mach numbers 6, 8, and 10 and a nominal Reynolds number of 1.0×10^6, based on model diameter.

CONTENTS

APPENDIXES

I. ILLUSTRATIONS

Figure

NOMENCLATURE

a	Speed of sound, in.-sec^{-1}
C_p	Pressure coefficient, $(p - p_\infty)/q_\infty$
M	Mach number
p	Pressure, psia
q_∞	Free-stream dynamic pressure, psia
R_n	Model nose radius, in.
Re_∞	Free-stream Reynolds number based on model diameter
S	Surface distance from model axis of symmetry, in.
T	Temperature, °R
u	Velocity, in.-sec^{-1}
γ	Test gas ratio of specific heats
θ	Angle between model axis of symmetry and a normal to the model surface, deg, or radians as noted

SUBSCRIPTS

ℓ	Model local or surface conditions
o	Tunnel stilling chamber conditions
s	Conditions at model stagnation point
∞	Free-stream conditions

SUPERSCRIPT

*	Sonic conditions

SECTION I
INTRODUCTION

The evolution of space flight has presented man with the problem of an atmospheric re-entry from orbital heights at extremely high speeds. Aerodynamic heating is one of the major problems encountered in re-entry flight. Limitations in the development of cooling techniques have precluded the use of the more aerodynamically desirable sharp-nose lifting configurations. All current and past United States manned space flight efforts (Mercury, Gemini, and Apollo) utilize spacecraft which present a blunt spherical shaped heat shield to the high energy flow experienced during re-entry.

Hypersonic convective stagnation heating has been shown theoretically by Fay and Riddell (Ref. 1) to be dependent on the square root of the surface velocity gradient at the stagnation point. Theoretical or experimental determination of the stagnation point velocity gradient is therefore required to predict the stagnation heating of a particular configuration.

Theoretical prediction of the pressure distribution, and therefore the velocity distribution, of hemispherical shaped bodies in hypersonic flow has been accomplished with considerable success using modified Newtonian theory as was demonstrated recently by Clark. However, as bluntness is increased beyond that of the hemisphere, the Newtonian prediction becomes less accurate. Several analytic and numerical solutions for the blunt body flow problem have appeared in the literature, for example Refs. 3 and 4. In spite of considerable analytic study of the problem, there are little hypersonic wind tunnel data available for substantiation of the theoretical work. The purpose of this study was to provide experimental data in the hypersonic flight regime (data were obtained at nominal Mach numbers 6, 8, and 10) suitable for correlation with existing theories. The tests were conducted in the AEDC von Kármán Facility's 50-in. hypersonic tunnels (Gas Dynamic Wind Tunnels, Hypersonic (B) and (C)).

A family of bodies with spherically blunted noses ranging in bluntness from the hemisphere to the flat-nose cylinder was studied (the flat-nose cylinder is considered a spherical segment of infinite radius). The manned spacecraft mentioned previously are members of this family. A similar study has been conducted at supersonic speeds (M_∞ = 2.01 to 4.76) by Boison and Curtiss (Ref. 5). Particular emphasis was given the stagnation point velocity gradient, or a form thereof, because of its importance in aerodynamic heating. Newtonian theory was used as a correlation basis for the data.

SECTION II
THEORETICAL ANALYSIS

It is well known that for simple applications, the Newtonian theory for the prediction of pressures acting on hypersonic vehicles is remarkably accurate. A thorough analysis of the development of this theory was given by Hayes and Probstein (Ref. 6), and an example of its utility and application was given in Ref. 7.

For the purpose of this study, a modified form of the Newtonian theory is used as shown in Eq. (1).

$$\frac{C_p}{C_{p_s}} = \cos^2 \theta \tag{1}$$

Use of the definition of C_p and algebraic manipulation gives

$$\frac{p}{p_s} = \cos^2 \theta + \frac{p_\infty}{p_s} \sin^2 \theta \tag{2}$$

Assuming an isentropic expansion of a perfect gas from a reservoir at the stagnation point of the model, $\frac{p}{p_s}$ may also be expressed as

$$\frac{p}{p_s} = \left(1 + \frac{\gamma - 1}{2} M_\ell^2\right)^{\frac{-\gamma}{\gamma - 1}} \tag{3}$$

Substitution of Eq. (3) into Eq. (2) gives

$$\left(1 + \frac{\gamma - 1}{2} M_\ell^2\right)^{\frac{-\gamma}{\gamma - 1}} = \cos^2 \theta + \frac{p_\infty}{p_s} \sin^2 \theta \tag{4}$$

Differentiation of Eq. (4) with respect to M_ℓ and θ considering $\frac{p_\infty}{p_s}$ and γ constant gives

$$\frac{dM_\ell}{d\theta} = \frac{\sin 2\theta \left(\frac{p_\infty}{p_s} - 1\right)}{-\gamma M_\ell \left(1 + \frac{\gamma - 1}{2} M_\ell^2\right)^{\frac{-2\gamma + 1}{\gamma - 1}}} \tag{5}$$

θ and M_ℓ are both zero at the stagnation point, and the derivative obtained in Eq. (5) is observed to be indeterminate for this condition. However, application of l'Hospital's rule to Eq. (5) and setting θ and M_ℓ equal to zero yields the usable form:

$$\left(\frac{dM_\ell}{d\theta}\right)_s = \left[\frac{2}{\gamma}\left(1 - \frac{p_\infty}{p_s}\right)\right]^{\frac{1}{2}} \tag{6}$$

In order to make Eq. (6) applicable to the experimental study, θ is represented in terms of arc length and nose radius giving

$$\left(\frac{dM_\ell}{dS}\right)_s = \frac{1}{R_n}\left[\frac{2}{\gamma}\left(1 - \frac{p_\infty}{p_s}\right)\right]^{1/2} \tag{7}$$

Nondimensionalizing S with the sonic arc length S* gives

$$\left(\frac{dM_\ell}{d\frac{S}{S^*}}\right)_s = \frac{S^*}{R_n}\left[\frac{2}{\gamma}\left(1 - \frac{p_\infty}{p_s}\right)\right]^{1/2} \tag{8}$$

Noting that $\frac{S^*}{R_n}$ is equivalent to θ^*, Eq. (8) is rewritten:

$$\left(\frac{dM_\ell}{d\frac{S}{S^*}}\right)_s = \theta^* \left[\frac{2}{\gamma}\left(1 - \frac{p_\infty}{p_s}\right)\right]^{1/2} \tag{9}$$

For an isentropic expansion of a perfect gas, $\frac{p_\infty}{p_s}$ is a function of M_∞ and γ. $\left(\frac{dM_\ell}{d\frac{S}{S^*}}\right)_s$ is, therefore, determined by θ^*, M_∞, and γ.

Conversion of the stagnation point Mach number gradient $\left(\frac{dM_\ell}{d\frac{S}{S^*}}\right)_s$ to the stagnation point velocity gradient as required by the Fay and Riddell heat-transfer theory (Ref. 1) is easily accomplished as shown in Eq. (10):

$$\left(\frac{du}{dS}\right)_s = \left(\frac{dM_\ell}{d\frac{S}{S^*}}\right)_s \left(\frac{a_s}{S^*}\right) \tag{10}$$

Calculation of θ^* by the Newtonian theory is accomplished by equating Eq. (2) to the sonic pressure ratio and solving for θ. The sonic pressure ratio is obtained from Eq. (3) by letting $M_\ell = 1$

$$\theta^* = \sin^{-1}\left[\frac{1 - \left(\frac{\gamma+1}{2}\right)^{\frac{-\gamma}{\gamma-1}}}{1 - \frac{p_\infty}{p_s}}\right]^{1/2} \tag{11}$$

Substitution of Eq. (11) into Eq. (9) would provide an equation for $\left(\frac{dM_\ell}{d\frac{S}{S^*}}\right)_s$ dependent on M_∞ and γ. It is important to note, however, that Eq. (11)

may not apply for a spherical nose segment which is terminated (or cut) at a θ less than the calculated θ^*. If the surface following the cut permits a flow expansion to sonic velocity at the cut, the sonic point location is fixed. In this case, the logical choice for θ^* in Eq. (9) is not the Eq. (11) value but the θ of the cut.

SECTION III
APPARATUS

3.1 MODELS

The four spherically blunted cylinder models used for the study are illustrated in Fig. 1. A photograph of the models is presented in Fig. 2. The models were constructed of stainless steel and were mounted in the wind tunnels by means of a sting supported base plate. The cylinder diameter of each model was 5.800 in., and the cylinder length varied from 4.00 in. for Model A to 5.20 in. for Model D. The model support sting diameter was 2.5 in.

Model A, the flat-nose cylinder, was instrumented with nineteen 0.067-in.-diam pressure orifices. Orifice spacing was in 0.145-in. intervals from the geometric center of the model to the nose-cylinder junction excluding the S = 0.145 and 2.900 points.

Model B, nose-to-cylinder radius ratio of 4, was instrumented with eight 0.040-in.-diam pressure orifices. Orifice spacing was in θ = 2-deg increments from the model geometric center (θ = 0) to θ = 14 deg. The nose-cylinder junction was at θ = 14.48 deg.

Model C, nose-to-cylinder radius ratio of 2, was instrumented with ten 0.040-in.-diam pressure orifices. Orifice spacing was in θ = 3-deg increments from the model geometric center (θ = 0) to θ = 27 deg. The nose-cylinder junction was at θ = 30 deg.

Model D, the hemisphere cylinder, was instrumented with ten 0.067-in.-diam pressure orifices. Orifice spacing was in θ = 10-deg increments from the nose geometric center (θ = 0) to θ = 90 deg at the nose-cylinder junction.

3.2 WIND TUNNELS

Tunnels B and C are continuous, closed-circuit, variable density wind tunnels with axisymmetric contoured nozzles and 50-in.-diam test sections. Tunnel B operates at a nominal Mach number of 6 or 8 at stagnation pressures from 20 to 300 and from 50 to 900 psia, respectively, at stagnation temperatures up to 1350°R. Tunnel C operates at a nominal Mach number of 10 or 12 at stagnation conditions from 200 to 2000 psia at 1900°R and 600 to 2000 psia at 2400°R, respectively. The model may be injected into the tunnels for a test run and then retracted for model cooling or model changes without interrupting the tunnel flow. A description of the tunnels may be found in Ref. 8.

3.3 INSTRUMENTATION

The basic measurements for this study were the model surface pressures. These pressures were measured with 15-psi differential transducers referenced to a near vacuum. Individual pressure orifices were selectively connected to the transducers by means of rotary valves. A pressure transducer and a thermocouple were used to measure the wind tunnel stagnation pressure and temperature, respectively. After analog-to-digital conversion of the measurements, data reduction was performed with an ERA 1102 digital computer.

SECTION IV
PROCEDURE

4.1 EXPERIMENTAL TECHNIQUE

Two basic problems are encountered in the experimental determination of stagnation point velocity gradients on blunt bodies. First, the velocity in the stagnation region is relatively low, and the pressure and velocity gradients are low compared to those of less blunt shapes. The result is that determination of small pressure gradients at relatively high pressure levels is required. Secondly, blunt model pressure distributions are distorted by relatively small free-stream flow nonuniformities in the area of the model nose. Several steps were taken to overcome these problems.

Model pressures in the stagnation region were recorded by a single pressure transducer, thereby essentially eliminating variations in indicated pressure levels caused by transducer nonlinearities and zero shifts between transducers.

Free-stream flow calibrations obtained from pitot pressure measurements were examined to determine test section regions of most nearly uniform flow. In some cases, flow calibrations were obtained immediately prior to the tests. These efforts enabled testing of the models in a free-stream flow uniform within 0.035 Mach number ($\Delta(p/p_s) = \pm 1$ percent). Further effort to nullify any remaining effects of free-stream flow non-uniformities was made by rolling the model about its axis to obtain data in several different planes. From five to seventeen sets of data were obtained for each model in this manner. These data were then averaged to provide the most likely model pressure distribution. Approximately 95 percent of all model pressure measurements fell within ±1 percent of the average values.

The tests were conducted at a free-stream Reynolds number of 1.0×10^6, based on model diameter, when possible. Some deviation from this condition was unavoidable because of wind tunnel operational problems. The data were obtained at zero angle of attack, that is, with the model axis aligned with the free-stream flow.

Test conditions are listed below:

TEST CONDITIONS

Model	M_∞	$Re_\infty \times 10^6$	p_o, psia	T_o, °R	p_s, psia
A	6.02	1.0	112	850	3.2
A	8.00	1.0	435	1290	3.7
A	10.12	0.8	1200	1845	3.4
B	6.02	1.0	112	850	3.2
B	8.00	1.0	435	1290	3.7
B	10.22	1.0	1700	1900	4.6
C	6.02	1.0	112	850	3.2
C	8.00	1.0	435	1290	3.7
C	10.22	1.0	1700	1900	4.6
D	6.03	1.3	150	850	4.3
D	7.99	0.9	400	1290	3.4

4.2 DATA PRECISION

Estimates of the precision of the results of this study are presented below:

DATA PRECISION

Measurement	Magnitude of Measurement	Estimated Error
p	1.5 to 4.6 psia	±0.5 percent
R_n	2.9 to 11.6 in.*	±0.005 in.
S	0 to 3.04 in.	±0.005 in.
T_s	850 to 1900°R	±1 percent
$\left(\frac{dM_\ell}{d\frac{S}{S^*}}\right)_s$	0.3 to 0.9	±0.02

*For Model A, $R_n = \infty$, and the error quoted applies to the deviation in flatness of the nose.

4.3 DATA ANLYSIS

Based on the Newtonian prediction of the hemisphere sonic point location, it was estimated that for Models A, B, and C the entire nose region flow would be subsonic. Also, since a sharp corner and a minimum expansion angle of 60 deg existed at the nose-cylinder junction, it was assumed that the sonic point for these models would be fixed at the corner. The Model D sonic point was expected to occur at a θ of about 42 deg. Considering, then, that the flow in the region of interest would be subsonic, a method of data analysis was sought. Boison and Curtiss (Ref. 5) used an incompressible approach to the problem; however, this restriction need not be imposed if the compressible flow relationships are used. Knowledge of the model surface pressure distribution allows a description of the nose region flow, providing the following assumptions are made:

1. The flow follows an isentropic expansion of a perfect gas from a reservoir at the stagnation point.
2. The static pressure is constant through the boundary layer in the direction normal to the model surface.
3. The stagnation or reservoir temperature is known.

The assumption of an isentropic expansion of a perfect gas from the stagnation point was verified experimentally by Crawford and McCauley (Ref. 9) by making near surface pitot pressure surveys on a hemisphere

at a free-stream Mach number of 6.8. Application of assumptions 1 and 2 permits conversion of the model surface pressure distributions to model surface Mach number distributions by means of the compressible flow tables (Ref. 10). As previously mentioned, the Model A, B, and C sonic points were assumed to be at the nose-cylinder junction. Location of a pressure orifice to verify this assumption was not mechanically practical. For Model D, however, the pressure data were plotted to determine the experimental sonic point location. The surface distance was nondimensionalized with the sonic distance S* for all models in order to avoid scaling effects in the data presentation.

Plotting the surface (or local) Mach number distributions as a function of $\frac{S}{S^*}$ permitted an examination of the effects of body contour without regard to scaling or temperature effects. Evaluation of the stagnation point Mach number gradient was accomplished by obtaining the slope of the M_ℓ versus $\frac{S}{S^*}$ curves at the stagnation point. Conversion of the stagnation point Mach number gradient $\left(\frac{dM_\ell}{d\frac{S}{S^*}}\right)_s$ to the stagnation point velocity gradient, as required for heat-transfer calculations (Ref. 1), may be accomplished as previously shown in Eq. (10).

As indicated in assumption 1, an isentropic expansion of a perfect gas has been assumed for the data presented. The test gas for this study was air, and the value used for γ was 1.4. For the present test conditions, the maximum error in local Mach number attributable to the perfect gas assumption would be less than one percent.

SECTION V
RESULTS AND DISCUSSION

Experimental pressure distributions obtained from Models A, B, C, and D are graphically presented in Fig. 3 and tabulated in Table I. All data presented represent average values obtained in the manner described in Section 4.1. Newtonian theory predictions are shown with each set of data and were calculated from Eq. (2) after converting θ to S/S*. As expected, agreement between the data and Newtonian theory was poor for Model A (Fig. 3a) and improved as bluntness decreased such that for Model D (Fig. 3d) the agreement was excellent. Calculations by Gold and Holt (Ref. 11) for the Model A pressure distribution at Mach number 5.8 using the Belotserkovskii method are shown in Fig. 3a and are in reasonable agreement with the data.

The Van Dyke prediction for the Model D pressure distribution (Fig. 3d) was obtained from calculations by C. H. Lewis of the von Kármán Facility and the calculation procedure was described in Ref. 12. This prediction is slightly lower than the Newtonian prediction but is also in excellent agreement with the data. Mach number effects on the model pressure distributions over the range tested were not apparent with the possible exception of Model B (Fig. 3b). The $M_\infty = 10$ data for this model were consistently higher than those obtained at $M_\infty = 6$ or 8. Model D Mach number 10 data were previously measured in Tunnel C and reported by Clark in Ref. 2. These data were used for the present study.

For Models A, B, and C the sonic point location was assumed to be geometrically fixed at the model shoulder; however, for Model D the sonic point was experimentally (and theoretically) determined. The sonic point was located by interpolation between data points at a value of $p/p_S = 0.528$. To aid in the use and interpretation of the Model D data, sonic point location as a function of Mach number is shown in Fig. 4. Data published by Kendall (Ref. 13) and Boison and Curtiss (Ref. 5) are included to provide continuity of the present results with lower Mach number (1.8 to 4.8) data. An empirical correlation from Ref. 2 along with Newtonian and Van Dyke sonic point location predictions are included in Fig. 4. The Van Dyke and empirical correlation values are in good agreement with the experimental results. The Newtonian prediction is high relative to the data and other results but does follow the general trend with Mach number. Mach number 1.82 data from Ref. 5 were obtained with a model which was terminated at $\theta = 0.785$ (45 deg), thereby apparently forcing the sonic point to occur at a θ less than that for a complete hemisphere.

Model local Mach number distributions as determined from the pressure data (Fig. 3) are presented in Fig. 5. The primary function of this data presentation was to permit evaluation of the stagnation point Mach number gradient $\left(\frac{dM_\ell}{d\frac{S}{S^*}}\right)_S$. Theoretical comparisons similar to those in Fig. 3 are included. Gradients were evaluated by measuring the slope of the data fairing at the stagnation point. Observation of the data will reveal that in some cases (particularly for Model A, Fig. 5a) it was necessary to essentially ignore some data points very near the stagnation point. The data irregularities were attributed to tunnel flow nonuniformity, and by weighting outboard readings more heavily, consistent gradients were obtained.

A correlation of the stagnation point Mach number gradients obtained from Fig. 5 with bluntness is presented in Fig. 6. The use of θ^* as a bluntness correlation parameter is suggested by Newtonian theory (see Eq. (9)). Although the level of the gradients $\left(\frac{dM_\ell}{d\frac{S}{S^*}}\right)_s$ was not accurately predicted by the theory, the data correlation was adequate to permit evaluation of gradients for shapes of arbitrary bluntness.

A comparison of the present test results with experimental results from supersonic tests (Refs. 5 and 13) is presented in Fig. 7. A small extrapolation of the Ref. 5 data was necessary to permit comparison with Models B and C. It is generally concluded that free-stream Mach number effects on the stagnation point Mach number gradient in the hypersonic flow regime were small and essentially within experimental precision.

An interesting observation is made by comparing the overall Mach number trends (M_∞ = 2 to 10) of the parameter $\left(\frac{dM_\ell}{d\frac{S}{S^*}}\right)_s$. The Model C and D data follow the trends predicted by Newtonian theory. It should be noted that although for these models the trends are opposite (because of the variable sonic point location of Model D), the agreement with Newtonian theory is obvious. For Models A and B, however, the trend is reversed; that is, $\left(\frac{dM_\ell}{d\frac{S}{S^*}}\right)_s$ generally decreases with Mach number. These data suggest that for this family of bodies a basic reversal in the reaction of the stagnation region flow to free-stream Mach number variation exists at a bluntness somewhere between that of Model B and Model C.

REFERENCES

1. Fay, J. A. and Riddell, F. R. "Theory of Stagnation Point Heat Transfer in Dissociated Air." Journal of the Aeronautical Sciences, Vol. 25, No. 2, February 1958, pp. 73-85.

2. Clark, E. L. Private Communication. Arnold Engineering Development Center, Arnold Air Force Station, Tennessee, December 1966.

3. Vaglio-Lauren, Roberto. "On the PLK Method and the Supersonic Blunt-Body Problem." Journal of the Aerospace Sciences, Vol. 29, February 1962, pp. 185-206.

4. Van Dyke, Milton D. and Gordon, Helen D. "Supersonic Flow Past a Family of Blunt Axisymmetric Bodies." NASA Technical Report R-1, 1959.

5. Boison, J. Christopher and Curtiss, Howard A. "An Experimental Investigation of Blunt Body Stagnation Point Velocity Gradient." American Rocket Society Journal, Vol. 29, February 1959, pp. 130-135.

6. Hayes, Wallace D. and Probstein, Ronald F. Hypersonic Flow Theory. Academic Press, New York, 1959.

7. Clark, E. L. and Trimmer, L. L. "Equations and Charts for the Evaluation of the Hypersonic Aerodynamic Characteristics of Lifting Configurations by the Newtonian Theory." AEDC-TDR-64-25 (AD431848), March 1964.

8. Sivells, James C. "Aerodynamic Design and Calibration of the VKF 50-Inch Hypersonic Wind Tunnels." AEDC-TDR-62-230 (AD299774), March 1963.

9. Crawford, Davis H. and McCauley, William D. "Investigation of the Laminar Aerodynamic Heat Transfer Characteristics of a Hemisphere-Cylinder in the Langley 11-Inch Hypersonic Tunnel at a Mach Number of 6.8." NACA Report 1323, 1957.

10. "Equations, Tables, and Charts for Compressible Flow." NACA Report 1135, 1953.

11. Gold, Ruby and Holt, Maurice. "Calculation of Supersonic Flow Past a Flat-Head Cylinder by Belotserkovskii's Method." AFOSR TN-59-199, March 1959.

12. Roberts, J. F., Lewis, Clark H., and Reed, Marvin. "Ideal Gas Spherically Blunted Cone Flow Field Solutions at Hypersonic Conditions." AEDC-TR-66-121 (AD637703), August 1966.

13. Kendall, James M., Jr. "Experiments on Supersonic Blunt Body Flows." Jet Propulsion Laboratory Progress Report No. 20-372, February 1959.

APPENDIXES

I. ILLUSTRATIONS

II. TABLE

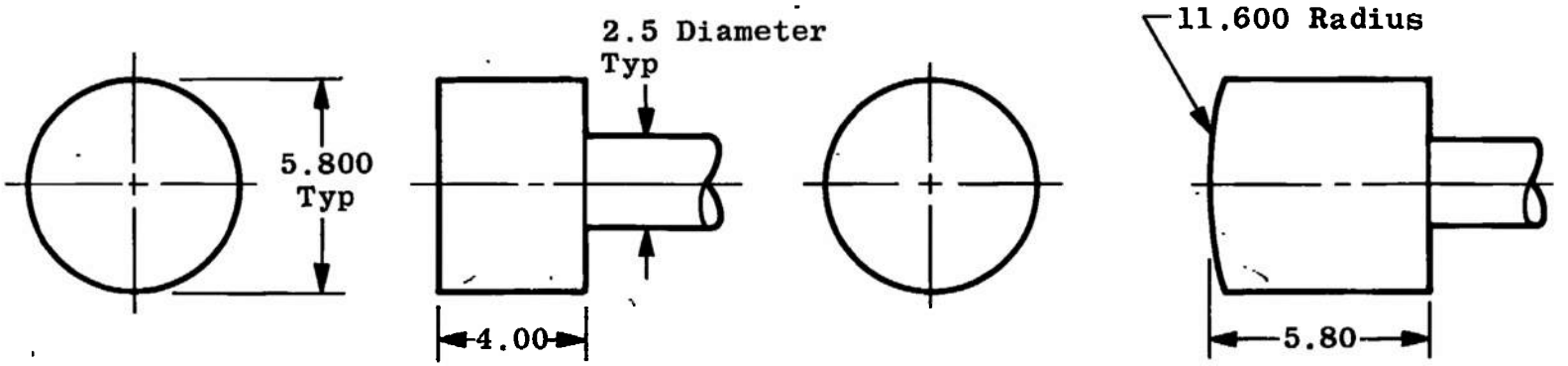

Model A

Model B

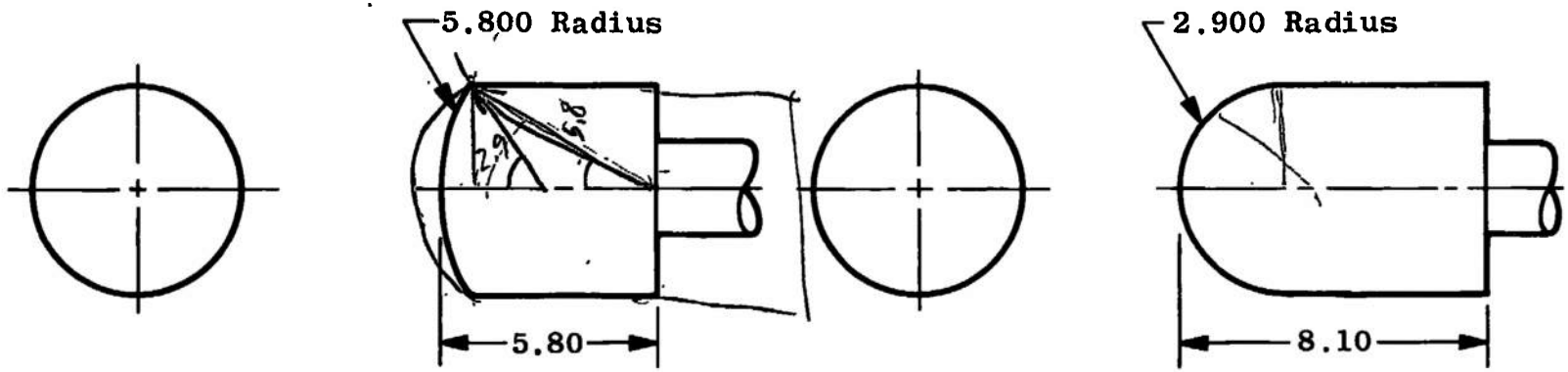

Model C

Model D

All Dimensions in Inches

Fig. 1 Test Models

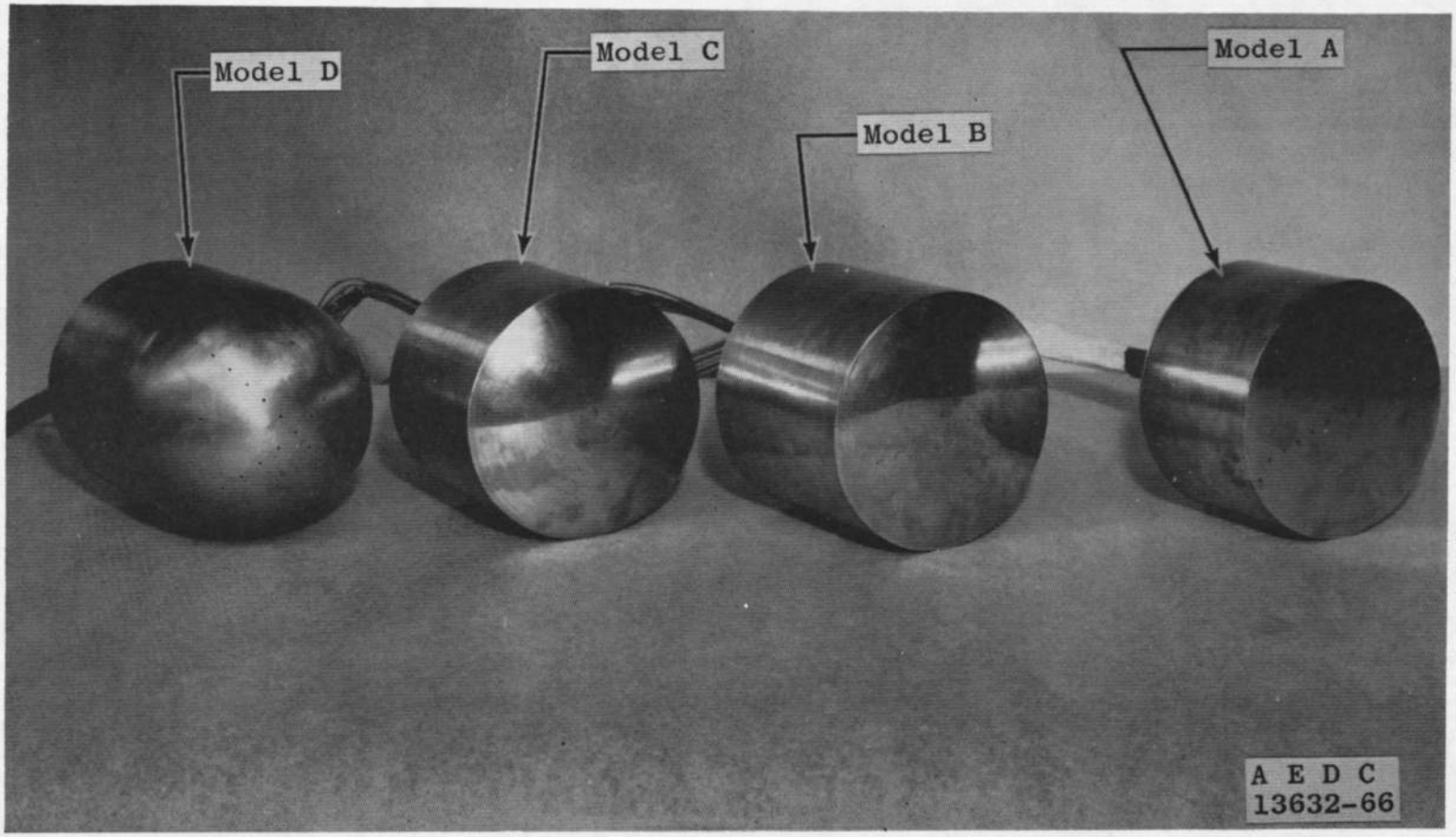

Fig. 2 Test Model Photograph

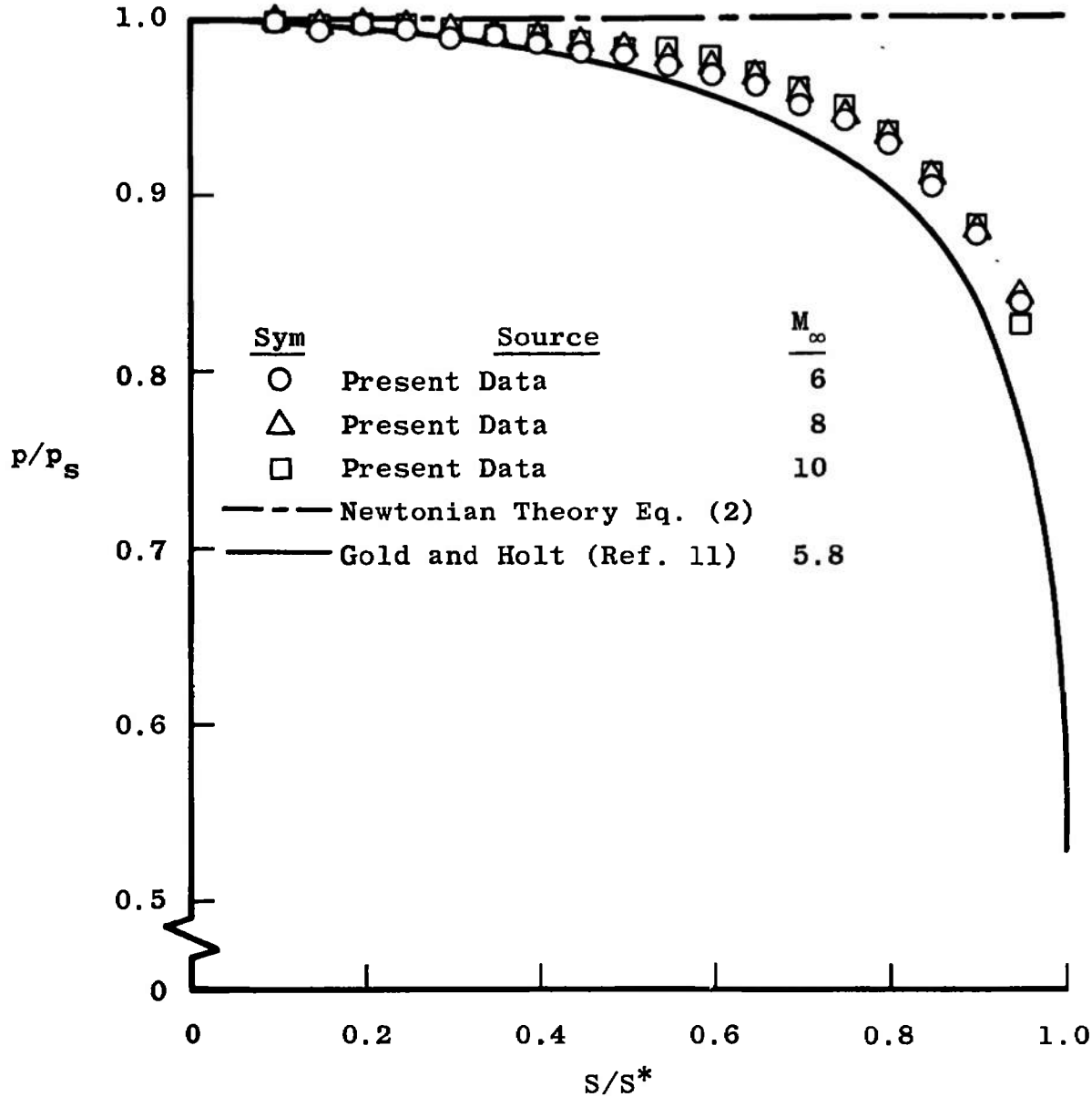

a. Model A

Fig. 3 Model Pressure Distributions

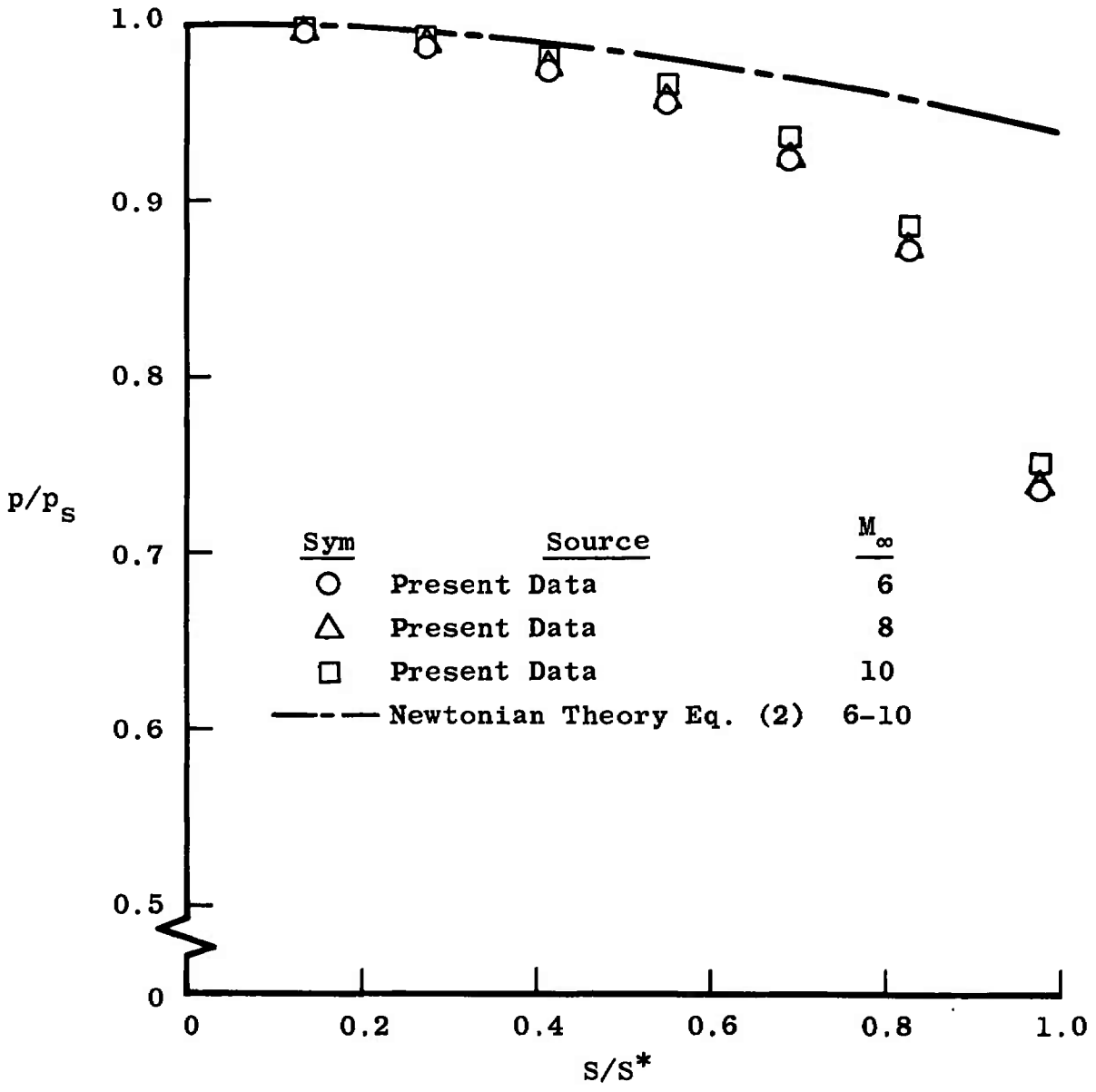

b. Model B

Fig. 3 Continued

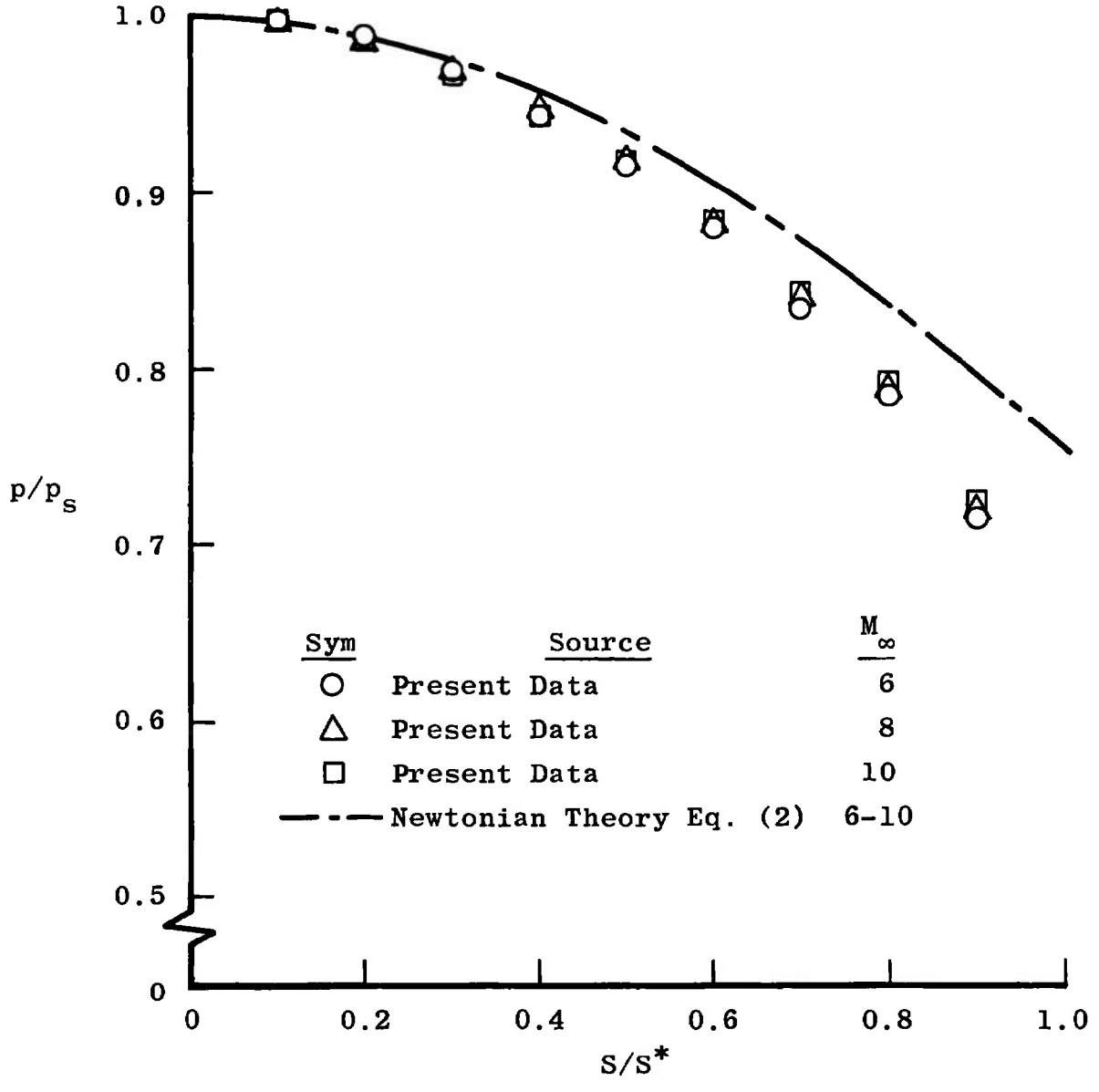

c. Model C

Fig. 3 Continued

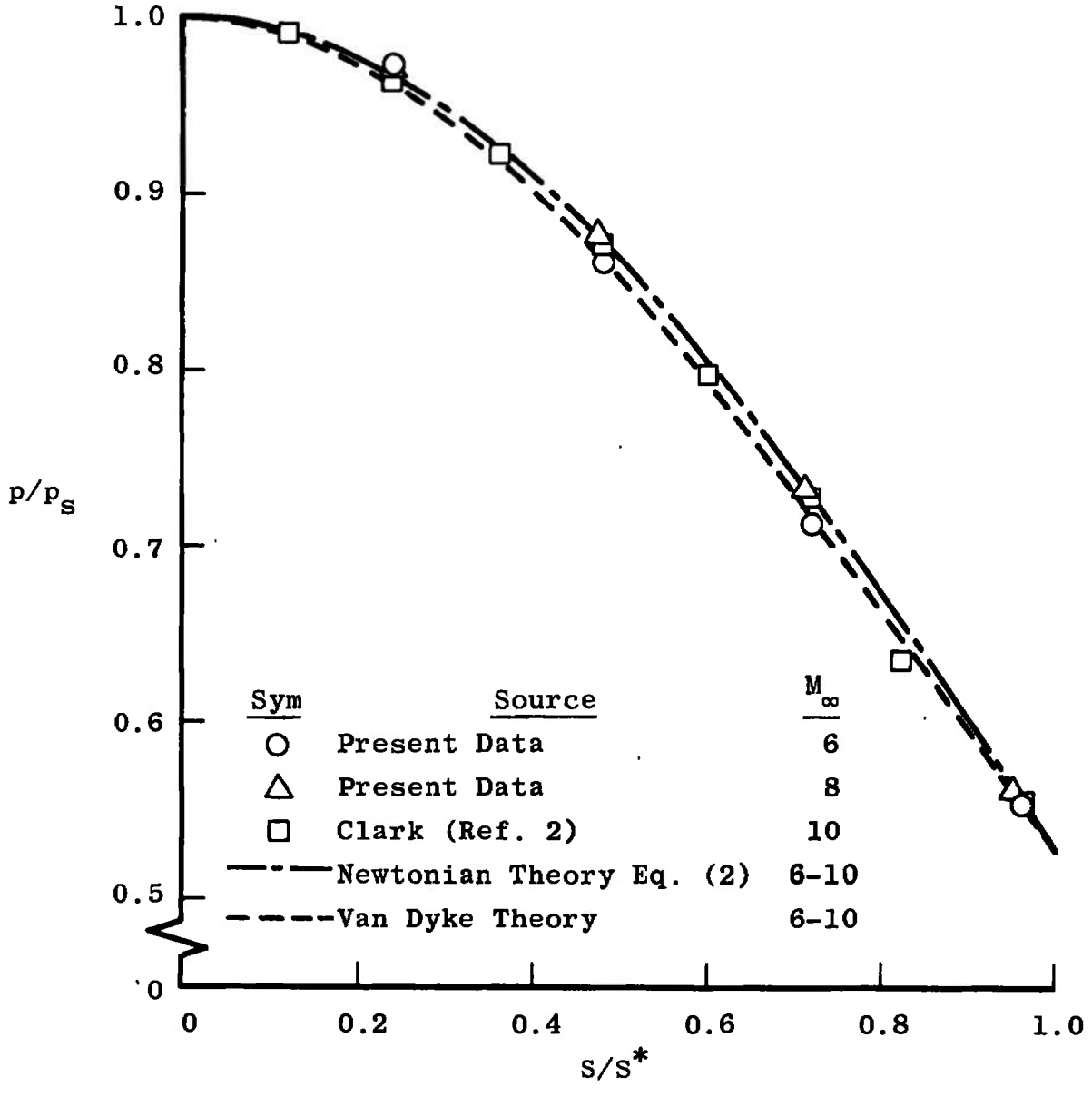

d. Model D

Fig. 3 Concluded

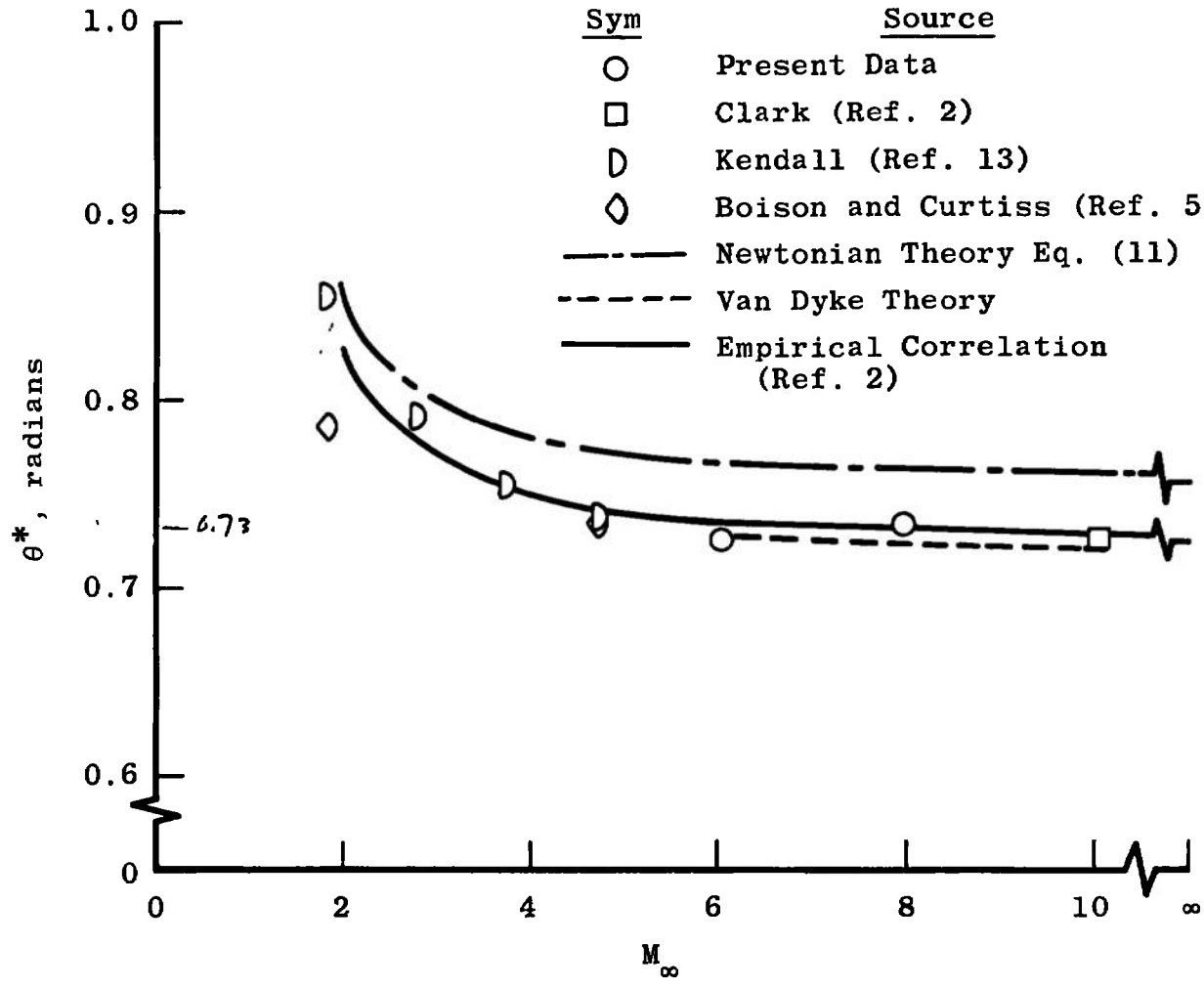

Fig. 4 Model D Sonic Point Location

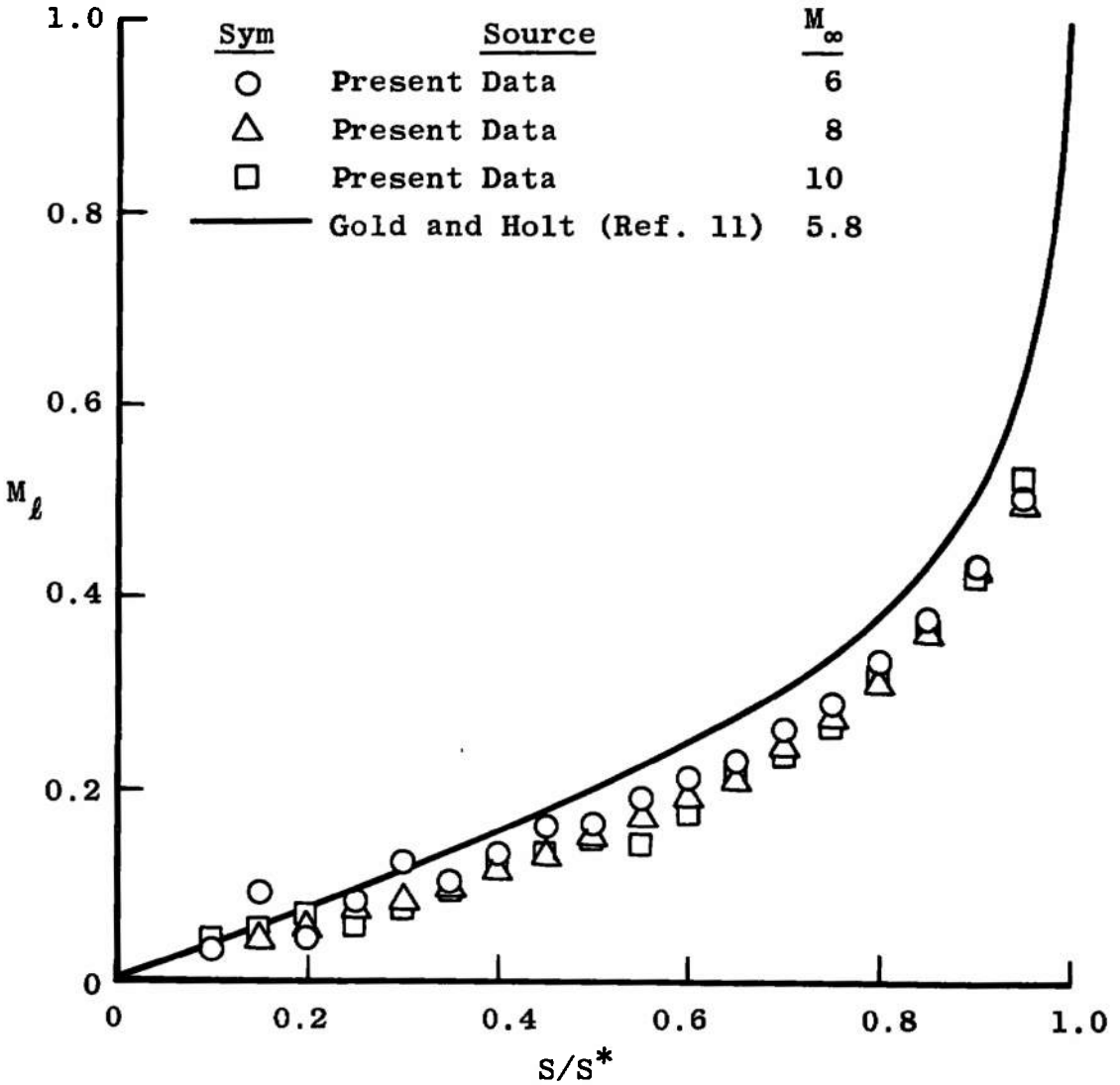

a. Model A

Fig. 5 Model Local Mach Number Distributions

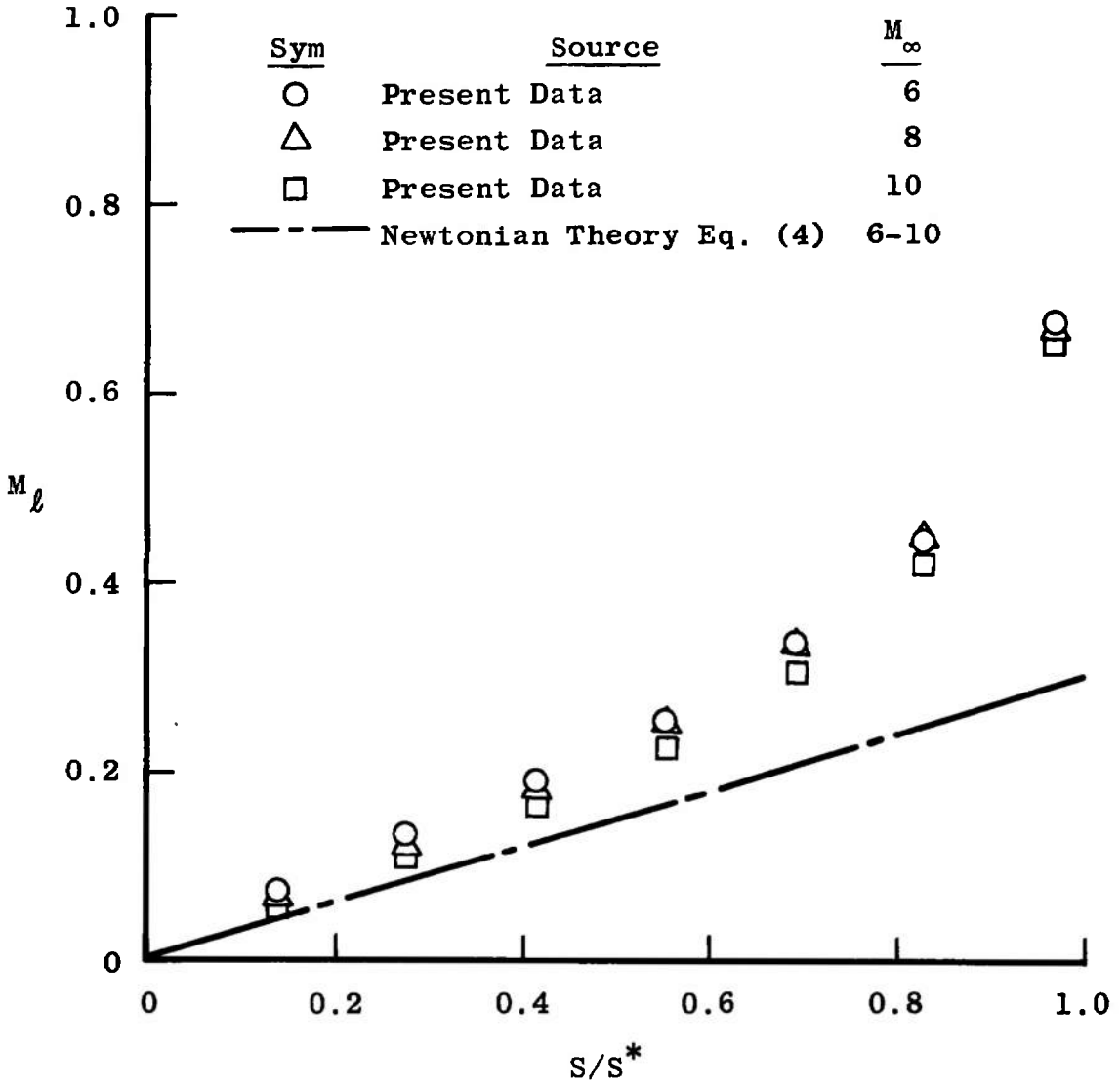

b. Model B

Fig. 5 Continued

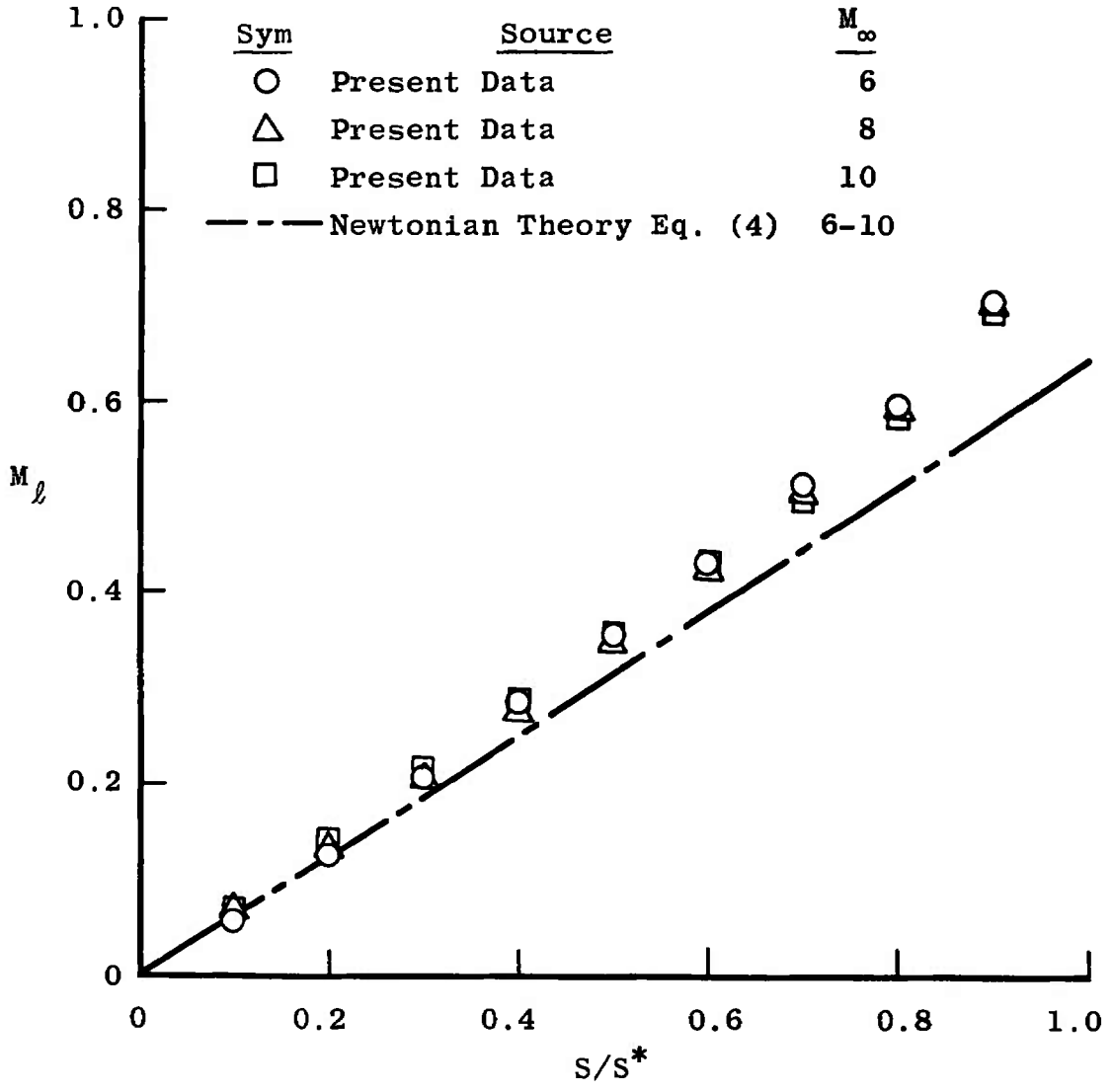

c. Model C

Fig. 5 Continued

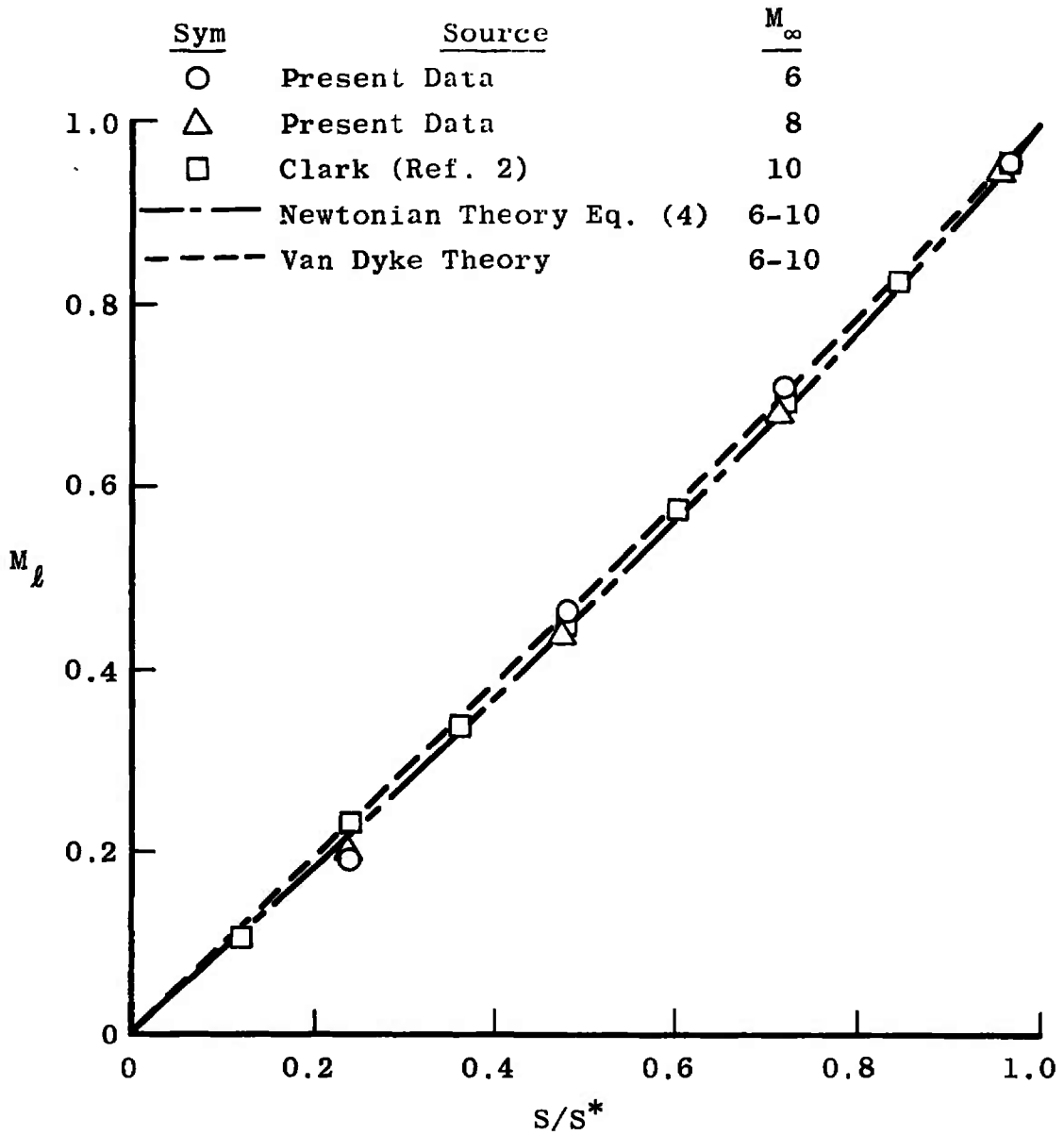

d. Model D

Fig. 5 Concluded

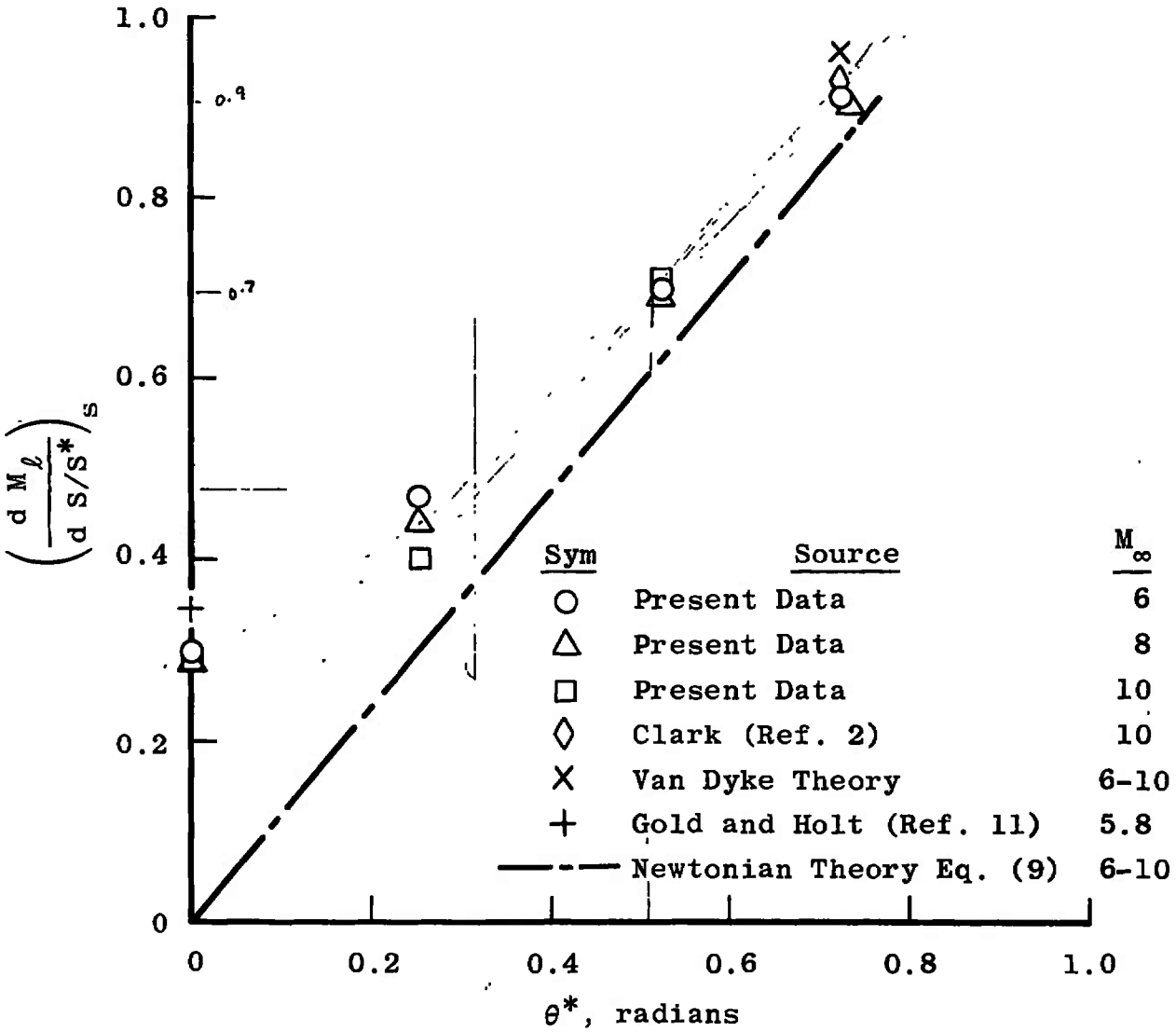

Fig. 6 Stagnation Point Mach Number Gradient Correlation with Bluntness

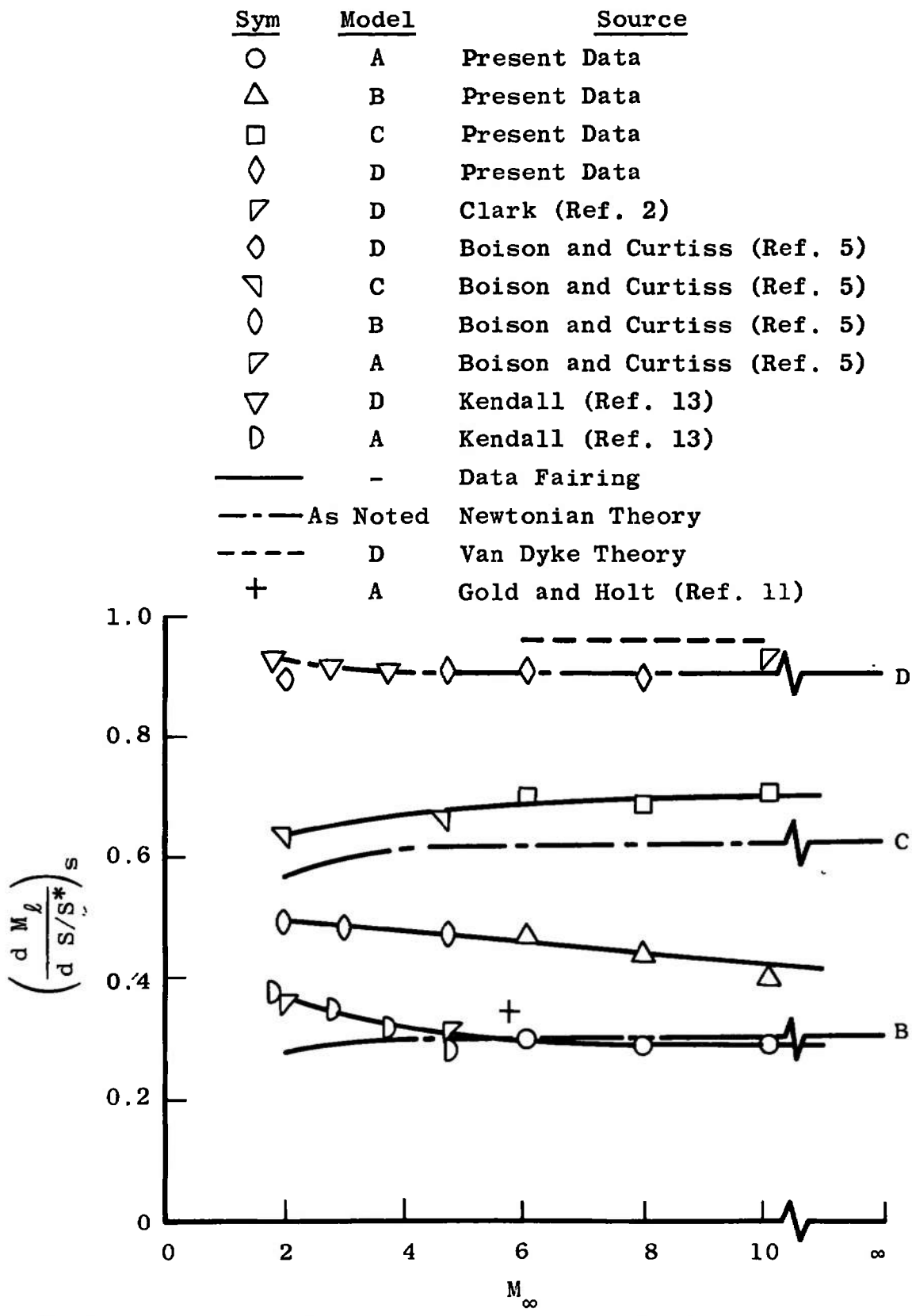

Fig. 7 Stagnation Point Mach Number Gradient Correlation with Free-Stream Mach Number

TABLE I
PRESSURE DATA TABULATION
Model A

θ, deg	S, in.	S/S*	$(p/p_S)_{M_\infty = 6}$	$(p/p_S)_{M_\infty = 8}$	$(p/p_S)_{M_\infty = 10}$
0	0	0	1.000	1.000	1.000
↓	0.29	0.10	0.999	0.999	0.999
	0.43	0.15	0.994	0.999	0.998
	0.58	0.20	0.998	0.998	0.997
	0.72	0.25	0.995	0.996	0.998
	0.87	0.30	0.989	0.995	0.996
	1.01	0.35	0.992	0.993	0.993
	1.16	0.40	0.987	0.990	0.991
	1.30	0.45	0.981	0.987	0.987
	1.45	0.50	0.980	0.984	0.983
	1.59	0.55	0.974	0.979	0.985
	1.74	0.60	0.968	0.974	0.979
	1.88	0.65	0.963	0.969	0.969
	2.03	0.70	0.952	0.958	0.961
	2.17	0.75	0.942	0.947	0.951
	2.32	0.80	0.929	0.935	0.934
	2.46	0.85	0.905	0.912	0.911
	2.61	0.90	0.877	0.880	0.883
	2.75	0.95	0.839	0.844	0.826
	2.90	1.00	---	---	---

TABLE I (Continued)
Model B

θ, deg	S, in.	S/S*	$(p/p_S)_{M_\infty = 6}$	$(p/p_S)_{M_\infty = 8}$	$(p/p_S)_{M_\infty = 10}$
0	0	0	1.000	1.000	1.000
2	0.40	0.14	0.996	0.997	0.996
4	0.81	0.28	0.986	0.990	0.987
6	1.21	0.41	0.971	0.977	0.978
8	1.62	0.55	0.952	0.956	0.963
10	2.02	0.69	0.920	0.924	0.936
12	2.43	0.83	0.870	0.871	0.883
14	2.83	0.97	0.733	0.740	0.742
14.48	2.93	1.00	---	---	---

Model C

θ, deg	S, in.	S/S*	$(p/p_S)_{M_\infty = 6}$	$(p/p_S)_{M_\infty = 8}$	$(p/p_S)_{M_\infty = 10}$
0	0	0	1.000	1.000	1.000
3	0.30	0.10	0.998	0.997	0.997
6	0.61	0.20	0.989	0.987	0.986
9	0.91	0.30	0.972	0.971	0.967
12	1.21	0.40	0.949	0.948	0.944
15	1.52	0.50	0.919	0.919	0.917
18	1.82	0.60	0.887	0.884	0.884
21	2.13	0.70	0.843	0.842	0.844
24	2.43	0.80	0.791	0.790	0.793
27	2.73	0.90	0.721	0.720	0.724
30	3.04	1.00	---	---	---

TABLE I (Concluded)
Model D

θ, deg	S, in.	$(p/p_s)_{M_\infty = 6}$	$(p/p_s)_{M_\infty = 8}$	$(p/p_s)_{M_\infty = 10}$ ①
0	0	1.000	1.000	1.000
5	0.25	---	---	0.992
10	0.51	0.974	0.972	0.963
15	0.76	---	---	0.923
20	1.01	0.862	0.876	0.871
25	1.26	---	---	0.798
30	1.52	0.713	0.732	0.727
35	1.77	---	---	0.637
40	2.02	0.554	0.562	0.555
45	2.28	---	---	0.467
50	2.53	0.396	0.395	0.388
55	2.78	---	---	0.312
60	3.04	0.260	0.255	0.252
65	3.29	---	---	0.194
70	3.54	0.158	0.154	0.152
75	3.80	---	---	0.114
80	4.05	0.089	0.085	0.085
85	4.30	---	---	0.062
90	4.55	0.049	0.047	0.046

M_∞	S*, in.
6	2.10
8	2.13
10	2.11

① Data from Ref. 2, $M_\infty = 10.05$, $Re_\infty = 0.63 \times 10^6$

Security Classification

DOCUMENT CONTROL DATA - R & D

(Security classification of title, body of abstract and indexing annotation must be entered when the overall report is classified)

1. ORIGINATING ACTIVITY (Corporate author)	2a. REPORT SECURITY CLASSIFICATION
Arnold Engineering Development Center ARO, Inc., Operating Contractor Arnold Air Force Station, Tennessee	UNCLASSIFIED
	2b. GROUP N/A

3 REPORT TITLE

STUDY OF THE BLUNT-BODY STAGNATION POINT VELOCITY GRADIENT IN HYPERSONIC FLOW

4 DESCRIPTIVE NOTES (Type of report and inclusive dates)

July 1966 Final Report

5. AUTHOR(S) (First name, middle initial, last name)

L. L. Trimmer, ARO, Inc.

6 REPORT DATE	7a. TOTAL NO. OF PAGES	7b. NO. OF REFS
May 1968	36	13

8a. CONTRACT OR GRANT NO	9a. ORIGINATOR'S REPORT NUMBER(S)
AF 40(600)-1200 b. PROJECT NO.	AEDC-TR-68-99
c. Program Element 6540223F d.	9b. OTHER REPORT NO(S) (Any other numbers that may be assigned this report) N/A

10 DISTRIBUTION STATEMENT

This document has been approved for public release and sale; its distribution is unlimited.

11 SUPPLEMENTARY NOTES	12. SPONSORING MILITARY ACTIVITY
Available in DDC	Arnold Engineering Development Center, Air Force Systems Command Arnold Air Force Station, Tenn.

13 ABSTRACT

Results of an experimental investigation to determine the stagnation point velocity gradients for a family of blunt axisymmetric shapes at hypersonic Mach numbers are presented. Data presented in the form of model pressure distributions and stagnation point Mach number gradients are compared with existing data and theories. Although not accurately predicting the results, Newtonian theory is shown to provide a good basis for data correlation. Variations in model pressure distribution and stagnation point Mach number gradient from free-stream Mach number 6 to 10 were small and essentially within experimental precision. Model bluntness ranged from a hemisphere-cylinder to a flat-nose-cylinder, and data were obtained at free-stream Mach numbers 6, 8, and 10 and a nominal Reynolds number of 1.0×10^6, based on model diameter.

DD FORM 1 NOV 65 1473

Security Classification

14 KEY WORDS	LINK A		LINK B		LINK C	
	ROLE	WT	ROLE	WT	ROLE	WT
hypersonic flow						
pressure distribution						
velocity gradients						
blunt bodies						